Journal of Materials Chemistry B

Accepted Manuscript

ROYAL SOCIETY OF CHEMISTRY

www.rsc.org/materialsB

Journal Name

RSCPublishing

ARTICLE

The Effect of Silk Gland Sericin Protein Incorporation into Electrospun Polycaprolactone Nanofibers on *in vitro* and *in vivo* Characteristics

Linhao Li,[a, b] Yuna Qian,[a] Chongwen Lin,[a] Haibin Li,[a] Chao Jiang,[a] Yonggang Lv,[a] Wanqian Liu,[a] Kaiyong Cai,[a] Oliver Germershaus,[b] and Li Yang [a, *]

Cite this: DOI: 10.1039/x0xx00000x

Received ooth January 2012,
Accepted ooth January 2012

DOI: 10.1039/x0xx00000x

www.rsc.org/

The application of silk fibroin is a promising approach for biomaterials design. However, silk sericin (SS) protein has not attracted much attention in the field of biomaterials as a natural biopolymer due to its immune responses, weak structural properties and high solubility. In this study, fifth instar silkworm (*B. mori*) middle gland extracted sericin protein and polycaprolactone (PCL) blends nanofibrous scaffolds were successfully fabricated via emulsion electrospinning technique. PCL/SS nanofibrous scaffolds were characterized by combined techniques of scanning electron microscopy (SEM), transmission electron microscopy (TEM), and Fourier-transform infrared spectroscopy (FTIR). Water contact angle and tensile measurements indicated that the PCL/SS scaffolds exhibited improved mechanical properties as well as more favorable wettability than that obtained from PCL alone. We also analyzed the effect of SS content in blends on cell morphology and proliferation of human primary skin fibroblasts (FEK4 cells) within 1-5 days. The results showed that cell proliferation significantly increased in the appropriate ratio of PCL/SS blends, while showing more elongated cellular morphology. The mRNA gene expression of transforming growth factor β1 (TGF-β1) and collagen I were up-regulated in PCL/SS scaffolds. Furthermore, *in vivo* experiments suggested that low fibrosis tissue formation and macrophages adhesion of the PCL/SS nanofibrous scaffolds reveal its potential as future biocompatible scaffolds for tissue engineering.

1. Introduction

Tissue engineering through the integrated use of cells, biomaterials/scaffolds and bio-regulatory agents represents a promising approach towards tissue repair or functional tissue replacements in regenerative medicine.[1, 2] The regeneration of functional tissue requires a suitable microenvironment that that closely mimics the host site for desired cellular responses. Cells are influenced by several cues that can drive from the structures, mechanical and chemical nature of the scaffolds. Therefore, one of the major challenges in regenerative medicine is to design and fabricate a suitable scaffold. With an ever-growing understanding of the interactions between cells and their environments in tissue, more attention is now given to fabricate scaffolds capable recapitulating key features of the extracellular matrix (ECM) that control cell migration, proliferation and differentiation.[3, 4] Native ECM is comprised of a complex network of structural and regulatory proteins arrayed into a nano-scale fibrous matrix. Recently, considerable efforts have been made to develop polymeric fibers mimicking ECM at sub-micron and nanometer scale. Nanofibrous scaffolds as synthetic ECM analogues are characterized by ultrathin continuous fibers, high aspect ratio, and interconnected porous structure with high porosity and variable pore size distribution, and result in altered or enhanced biological responses.

Polymeric nanofibers can be fabricated using a number of processing techniques including self-assembly,[5, 6] phase separation,[7] and electrospinning.[8] Among these, Nanofibrous scaffolds fabricated by electrospinning technology have enormous potential for tissue engineering applications. Electrospinning is a simple, versatile, and scalable technique to fabricate nanofibers from a wide range of polymers and polymer composites.[9, 10] Recently, a variety of natural and synthetic biodegradable polymers, including collagen, gelatin, chitosan, silk fibroin, poly (lactic acid) (PLA), poly (D, L-lactide-co-glycolide) (PLGA), and polycaprolactone (PCL), have been successfully electrospun to form nanofibrous scaffolds for different tissue engineering applications.[11-14] The composition of electrospun nanofibers derived from natural and synthetic polymers, combination the cell-friendly properties of the natural and mechanical strength of the synthetic polymers, represents an emerging class of nanostructures biomaterial scaffold.[15]

Silk fibers are fibrous protein with remarkable mechanical properties produced by silkworms and spiders. These proteins are produced within specialized glands known as silk glands after biosynthesis in the epithelial cells prior to spinning.[16, 17] Silk contains two natural macromolecular proteins–the fibrous fibroin protein and the water-soluble, glue-like sericin protein. Silk fibroin (SF) has been established as an attractive biomaterial for tissue engineering.[13, 18-20] Silk sericin (SS) also exhibits various biological properties that make it a potential candidate in pharmacological,

biomedical, and biotechnological field. Sericin protein shows antibacterial, antiapoptotic and ultraviolet resistant that attributes its use in skin care as cosmetics.[21, 22] SS also supports adhesion and proliferation of cells when used as a constituent of cell culture in serum-free media.[23-25] Zhang et al. reported that SS for surface modification of Ti promoted osteoblast cells adhesion, proliferation, and alkaline phosphatase activity.[26] Moreover, blends of various natural and synthetic polymers with SS allow to fabricated membranes, three-dimensional scaffolds, and hydrogels for tissue engineering applications.[27-31] On the other hand, the method of extraction significantly affects biochemical activities of silk proteins. The SS protein extraction with hot alkaline solution is now the most widely used degumming technique. However, this process makes it very difficult to gain high quality SS protein for further studies or applications. Alkali impurities also need to be removed before further extraction and purification.[32]

For ensuring electrospinning and structural stability, we presented a SS-based nanofibrous scaffolds based on blending with PCL, using emulsion electrospinning procedure. PCL has been widely used as synthetic polymer of choice in electrospun fibers owing to its excellent electrospinnability, favorable mechanical properties, good blend-compatibility, and slow degradation.[33] Since the SS protein would be denaturation in the high-temperature alkaline extraction process and thus affects the biochemical activities.[34, 35] In our previous study, we found that electrospun PCL/SS nanofibers have been limited by that lack of stable electrospun solution system and denaturation structures of SS under traditional extraction method.[36] In this study, therefore, we have used the native state of sericin protein, obtained through fifth instar silkworm *Bombyx mori* middle gland dissection, so that investigated the fabrication of using silk gland SS protein and PCL nanofibrous scaffolds with improved bioactivities by emulsion electrospinning. Thus, we hypothesized that PCL acted as the main structural and electrospinnable component of the scaffolds, while gland SS protein provided bioactivity for cell adhesion, proliferation and ECM production. The objectives of the study were to optimize the fabrication of PCL/SS nanofibrous scaffolds and to characterize material properties and *in vitro* cell responses, as well as evaluating the biocompatible properties with *in vivo* tests.

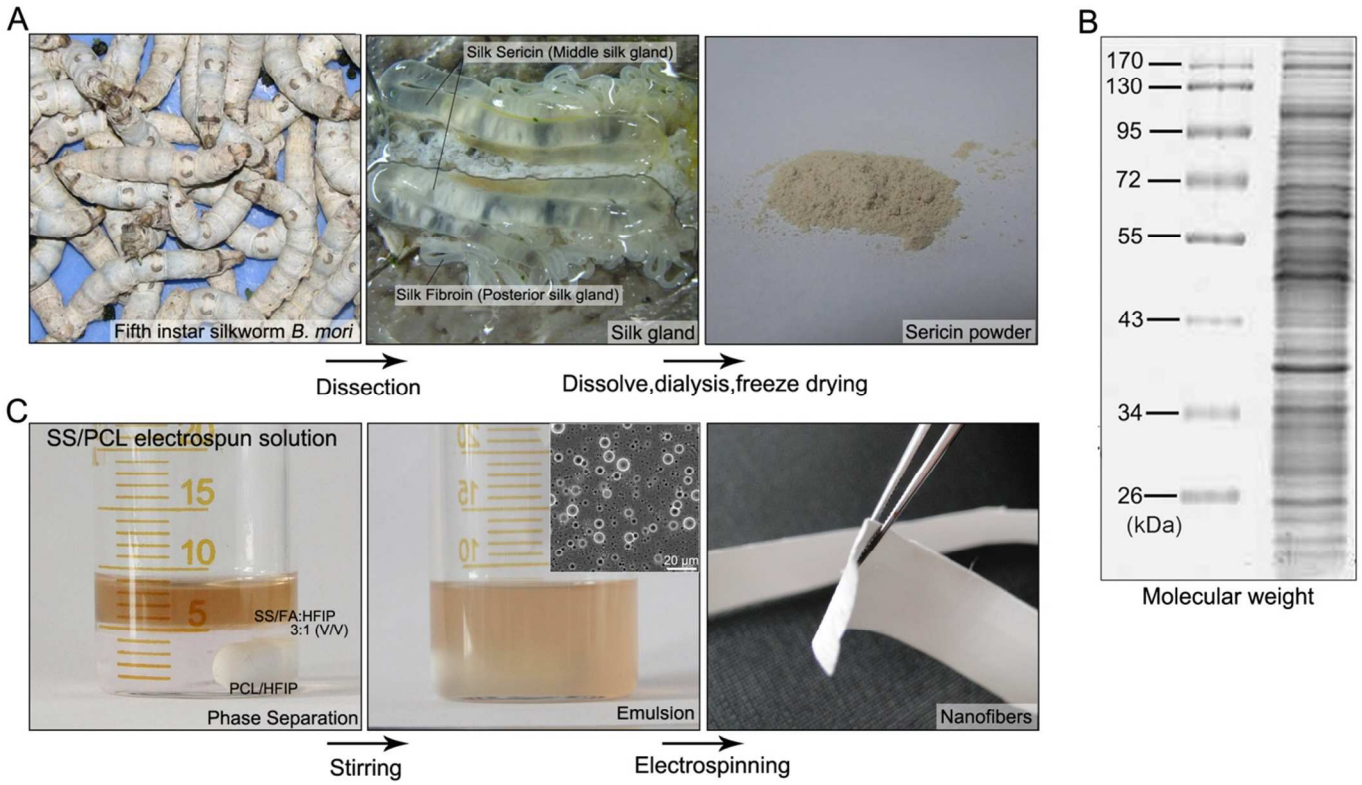

Figure 1. Schematic illustration of the procedure to extract silk middle gland sericin protein for fabricating PCL/SS nanofibrous scaffolds via emulsion electrospinning. (A) Protein extraction process. (B) Molecular weight of sericin protein as analyzed by SDS PAGE. (C) Emulsion electrospun PCL/SS nanofibrous scaffolds.

2. Experimental section

2.1. Materials and reagents

PCL (Mw = 80-90 kDa) was obtained from Sigma-Aldrich, Co. (St. Louis, MO, USA). Fifth instar *Bombyx mori* (silkworm) was obtained from Beibei Silkworm Egg, Co. (Chongqing, China). Hexafluoroisopropanol (HFIP) and formic acid (FA) were purchased from Dupont Chemical Co. (USA). Cellulose dialysis tubing (Mw = 3500 Da) were purchased from Pierce Chemical, Co. (USA). Fibroblasts media, RPMI 1640 medium, Dulbecco's Modified Eagle's Media (DMEM), fetal bovine serum (FBS) and antibiotics were purchased from Gibco LifeTechnology, Co. (USA). CellTiter 96-Aqueous One Solution Reagent (MTS), used in the cell proliferation assay, was purchased from Promega Co. (USA). Mouse monoclonal anti-CD68 antibody was purchased from Santa Cruz Biotechnology, Inc. (#sc-5299). Unless otherwise specified, all other reagents were purchased from Sigma-Aldrich.

2.2. PCL/SS emulsion electrospinning

2.2.1. Extraction of silk sericin protein from middle glands of silkworm

The fully-grown 5th instar larvae were dissected for extraction of silk sericin protein (**Fig. 1A**). SS was isolated from the silkworms just prior to spinning into cocoons. In brief, the middle silk glands were taken out and washed in Milli-Q water (Millipore Milli-Q system) to remove traces of body fluid. After keeping in water, the outer silk protein glandular tissue softens and swells, thus releasing the viscous silk SS sericin protein in water. The glandular tubes are then squeezed with fine forceps to extrude out the protein. The protein was collected in aliquots and kept at –20 ºC.

2.2.2. Preparation of electrospun solutions

SS protein were lyophilized and dissolved in 9.3 M LiBr at 55 ºC to generate a 10% (w/v) solution. This solution was dialyzed (Mw= 3500 Da) against UP water for 3 days by changing water daily to remove the ions and other impurities. The solution was collected, filtered and lyophilized to obtain SS powder. The molecular weight of gland SS protein was assessed by SDS-polyacrylamide gel electrophoresis (SDS-PAGE) using NuPAGE 4-12% Bis-Tris gels with MES running gel buffer at 150 V for 3 h. Gels were stained with commassie blue. Bands were scanned using a densitometer (GS-800; Bio-Rad, CA) (**Fig. 1B**).

PCL solution was prepared by dissolving 0.5 g of PCL in 5 mL HFIP to form 10% (w/v) solution. SS solution was prepared by dissolving 0.5 g of SS in 5 mL of FA/HFIP (volume 3:1) solution (10% (w/v)) under constant stirring at room temperature for 3 days. Six different solutions were prepared by mixing PCL and SS solution in ratios of 10: 0, 9: 1, 8: 2, 7: 3, 6: 4 and 5: 5 (v/v). For light microscopy, 0.1 mL emulsion droplet was dropped on a glass slide and observed with an inverted light microscopy (Olympus, IX71). Images were taken with the installed software (**Fig. 1C**).

2.2.3. Electrospinning

Electrospinning was performed in a fume hood using open cage target to collect fibers. Relative humidity was adjusted by flushing the hood with dry air. A volume flow rate of 1 mL/h of the electrospun solutions through a blunted stainless steel needle (ID = 0.8 mm) was maintained using a syringe pump (Longer Precision Pump, Baoding, China). For electrospinning, a range of voltage of 15-20 kV was applied to the capillary tube using a high voltage power supply (Dongwen High Voltage Power Supply Plant, Tianjin, China). The distance between the capillary tube and the grounded target was 12–15 cm. Random oriented fibrous scaffolds were collected on the open cage target of d = 15 cm when rotating at 300 min^{-1}.

2.3. Characterization of nanofibrous scaffolds

2.3.1. Field emission scanning electron microscopy (FESEM)

The morphology of nanofibrous scaffolds was characterized by FESEM (Zeiss Auriga crossbeam system, Germany) with an accelerating voltage of 5 kV after coating with gold. The diameter of the fibers was measured from the SEM images using image analysis software (Image J, National Institutes of Health, USA) and calculated by selecting 100–150 fibers SEM images randomly.

2.3.2. Transmission electron microscopy (TEM)

In order to detect internal structure properties, the fibers were prepared for TEM (Tecnai 12, FEI, Holland) by directly depositing the samples onto a copper grid, which was coated in advance with a supportive formvar film followed by a carbon coating. It was operated at 120 kV.

2.3.3. Fourier-transform infrared spectroscopy (FTIR)

Chemical analysis of SS powder and PCL/SS nanofibrous scaffolds were performed by Fourier-transform infrared (FTIR) spectroscopy over a range of 2000–1000 cm^{-1}. FTIR spectra of different samples were obtained by a Nicolet spectrometer system (System 2000, Perkin-Elmer) with a DTGS KBr detector. Around 1 mg of dried sample was mixed with 100–120 mg of KBr and compressed into pellets.

2.3.4. Water contact angle measurement

For determination of hydrophilicity of scaffolds, water contact angles of electrospun scaffolds were measured by a Model 200 video based optical system (Future Scientific Ltd. Co., Taiwan, China). The images of water drops on the sample surface were recorded by a camera, and then analyzed with software supplied by the manufacturer. Six samples were measured in each group. Three different points were measured for each sample. The initial distilled water volume of 5 µL was used in each measurement after 3 s exposure at ambient temperature.

2.3.5. Mechanical testing

Mechanical properties of different scaffolds were determined using a tabletop uniaxial testing instrument (Instron 5567, USA) using a 50-N load cell under a cross-head speed of 10 mm/min at ambient conditions (RH ~70%). All samples were prepared in the form of rectangular shape with dimensions of 40 mm × 20 mm × 200 µm (L × W × T) from the electrospun nanofibrous scaffolds. At least four samples were tested for each type scaffold. From the stress-strain curves, tensile strength and elongation at break were obtained.

2.4. Cell culture

The normal human skin primary fibroblast cells FEK4 (kindly supplied from Dr. RM Tyrrell's Lab, University of Bath, UK) were derived from a newborn foreskin explants. FEK4 cells were cultured in RPMI 1640 medium supplemented with 10% FBS, and 1% penicillin/streptomycin. After reaching 70% confluence, the cells were detached by trypsin–EDTA and viable cells were counted by hemocytometer. The nanofibrous scaffolds were immersed in 70% ethanol for 30 min, dried under sterile conditions and exposed to UV radiation for 1 h, washed 3 times with PBS for 20 min each and incubated with DMEM (serum free) for 24 h before cell seeding. Cells were further seeded onto nanofibrous scaffolds, placed in a 24-well plate at a density of 1×10^4 cells/well and cultured with DMEM and 10% FBS mixture at 37 ºC, 5% CO_2 and 95% humidity.

2.5. Cell morphology and proliferation

The morphology of FEK4 cells on PCL and PCL/SS nanofibrous scaffolds was observed by FESEM. After 1, 3 days of cell seeding, samples were fixed with 3% glutaraldehyde for 1 h. Specimens were rinsed in water and dehydrated with graded concentrations (50, 70, 90, 100% (v/v)) of ethanol. Subsequently the samples were treated with hexamethyldisiloxane (HMDS) and kept in a fume hood for air drying. Finally the samples were coated with gold for the observation of cell morphology.

To study the cell proliferation on different scaffolds, viable cells were determined by using the colorimetric MTS assay. The principle of this assay is that the reduction of yellow tetrazolium salt in MTS forms purple formazan product by the dehydrogenase enzymes secreted by mitochondria of the metabolically active cells. The absorbance of the formazan dye is measured at 490 nm and the amount of formazan crystals formed is directly proportional to the number of live cells. At first, we developed the standard curve to test cell proliferation in different scaffolds. The absorbance of six known cell numbers 10,000, 20,000, 40,000, 60,000, and 80,000 were used to construct a standard curve to convert absorbance readings to cell numbers. After 1, 3 and 5 days of cell seeding in 24-well plate, cells were washed with PBS and incubated with 20% of MTS reagent containing serum free medium. After 3 h of incubation at 37 ºC in 5 % CO_2, aliquots were pipetted into a 96-well plate. The absorbance of the content of each well was measured at 490 nm using a spectrophotometric microplate reader (Model 680, Bio-Rad).

2.6. RNA extraction and the real time RT-PCR

Real time RT-PCR was performed to determine the mRNA levels of collagen types I and III, and TGF-β1. Cells were detached using 0.25% trypsin solution and collected after brief centrifugation. Total RNA was isolated from the collected cells using a RNeasy Mini Kit (Qiagen Inc., USA) and then reverse transcribed into cDNA with a RevertAid^{TM} First Strand cDNA Synthesis Kit (#K1622, Fermentas, EU) according to the manufacturer's protocol. The sequences of forward and reverse primers were shown in Table 1 (primers were synthesized by Sangon Biotech Co., Ltd, Shanghai, China). GAPDH was detected as an internal control.

The real-time PCR reactions were performed using a fluorescence quantitative PCR detection system (Bio-Rad, USA). For each gene, PCR reactions were ran in a 25 μl mixture consisting of SYBR Premix Ex Taq (containing DNA polymerase, dNTP, reaction buffer and SYBR Green; DRR041A, TaKaRa Biotechnology Corp., Japan), cDNA and equal amounts of forward and reverse primers. PCR reaction conditions were 2 min at 50 ºC, 10 min at 95 ºC, and then 50 cycles at 95 ºC for 15 s, and 1 min at 60 ºC. Relative gene expression data was analyzed using the $2^{-\Delta\Delta C}{}_T$ method. Each sample was analyzed in triplicate.

Table 1
Primers for qPCR

Gene name	Forward primer (5' to 3')	Reverse primer (5' to 3')
Collagen I	TCTCCACTCTTCAGTTCCT	TTGGGTCATTTCCACATGC
Collagen III	TATTATAGCACCATTGAGA	TTATAAACCAACCTCTTCCT
TGF-β1	CCATACATTCCACATACTCCCACC	CCACAGTTCCACAGCAGTCCTC
GAPDH	GCACCGTCAAGGCTGAGAAC	TGGTGAAGACGCCAGTGGA

2.7. Subcutaneous implantation

The scaffolds were prepared in square shape with dimensions of 15 mm × 15 mm × 200 μm (L × W × T) under sterile conditions. 3-month-old male Sprague Dawley (SD) rats (body weight 230–250 g) were individually housed in wire bottom cages in temperature- and light-controlled rooms. All animals were allowed to acclimate to the housing facility for 5–7 days prior to intervention and had ad libitum access to food and water. The use of rats conformed to the Guiding Principles in the Care and Use of Animals for our Institute, and was approved by the Animal Care and Use Committee of our Institute. The animals were anaesthetized with 0.3% pentobarbital sodium (0.5 mL/100 g). We made three small midline incisions on the dorsum of the rat, and the scaffolds were introduced in lateral subcutaneous pockets created by blunt dissection. Procaine penicillin (20 mg/kg) was given intramuscularly preoperatively and after the operation for prophylactic infection control. Both animals remained in good general health throughout the study, as assessed by their weight gain. After 4 weeks, rats were sacrificed, and the implanted scaffolds were removed en bloc with the surrounding tissue naturally. The samples were fixed and processed for histology as described below.

2.8. Histology and immunohistochemistry

For histological evaluation, implantation sites were harvested 4 weeks post-surgery and fixed in 4% PFA for 48 h at 4 ºC. Samples were dried through a series of graded alcohol baths and in xylene, embedded in paraffin and sectioned in 10 μm thick slices. Sections were stained with Haematoxylin and Eosin (Beyotime, China). For immunohistochemistry using a monoclonal anti-CD68 antibody for rat macrophages, paraffin embedded sections of tissue exposed to films were deparrafinized through a series of graded alcohols, and treated with Trypsin for 30 min. The primary antibody was added to each slide and incubated overnight at 4 ºC in a humidified chamber. The secondary antibody was applied, carrying horseraddish peroxidase and developed according to the manufacturer's protocol (IHC staining module, Beijing Zhongshan Biotechnology, China). Sections were counterstained using hematoxylin for 5 min. Three samples for each group were analyzed by an inverted light microscope (Olympus, IX71).

2.9. Statistical analysis

Results are expressed as means ± standard deviations. Statistical analysis was performed using Student's t-test as well as one-way analysis of variance (ANOVA) followed by the Tukey's HSD (honestly significant difference) test for post hoc comparison (OriginLabOriginV8.0 Software). Difference was considered significant when $p < 0.05$.

3. Results and discussion

The experimental scheme used in this study is illustrated in Fig. 1 and mentioned in Section 2. In general, the SS would be denaturation in the high-temperature extraction process.[34] In order to maintain the activity and mechanical stability of sericin protein, we used the anatomy of the middle silk gland protein extraction. The SDS-PAGE pattern (Fig. 1B) of the SS solution exhibited clear bands at 0–180 kDa, showing that the solution contained small molecular weight sericin protein. The freeze-dried SS powder was dissolved in a mixture solvent of FA/HFIP (3:1 v/v), while PCL was dissolved in a solvent HFIP. After gentle stirring for 1 day, all the 91, 82, 73, 64, and 55 PCL/SS (w/w) solutions could be kept their homogeneous emulsion states for several days. Addition of slight HFIP in SS/FA solution as surfactants can improve compatibility of PCL/HFIP phase within the SS/FA phase.[37]

3.1. Emulsion electrospun PCL/SS nanofibrous scaffolds

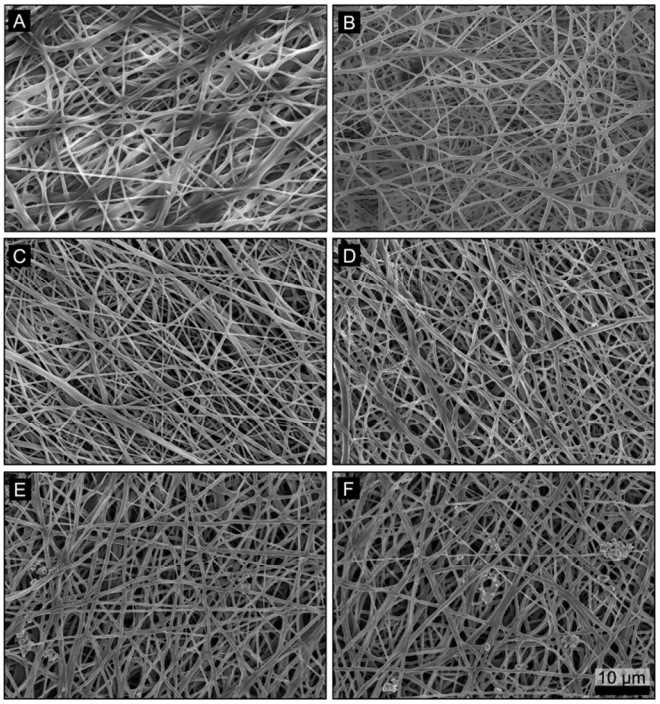

Figure 2. FESEM images of the electrospun PCL/SS blend scaffolds with different weight ratios: (A) PCL; (B) PCL/SS 91; (C) PCL/SS 82; (D) PCL/SS 73; (E) PCL/SS 64; (F) PCL/SS 55.

For electrospinning technology, many parameters influenced on the morphology and diameter of fibers, such as solution parameters (e.g. viscosity, conductivity, surface tension) and processing parameters (e.g. applied voltage, flow rate, needle diameter and spinnerent-collector distance).[10, 38, 39] Additionally, the solvent used to dissolve polymer has a significant effect on the spinnability of a polymer solution and the fiber morphology.[40, 41] Prior to this study, electrospun PCL/SS nanofibrous scaffolds have been successfully fabricated by our group. However, due to the heterogeneity of solution system, we found that the morphology, structures and mechanical properties of PCL/SS nanofibers were not uniform and stable.[36] Therefore, it was necessary to establish appropriate SS electospinning conditions. Hybrid PCL/SS nanofibrous scaffolds were fabricated under optimized electrospinning conditions in this study (Table 2). Here, HFIP/FA blend solvent was used as a good solvent to dissolve both SS and PCL. Water contact angle parameter was also analyzed for all the nanofibrous scaffolds as shown in Table 2. It was found that PCL nanofibers were hydrophobic having a contact angle of 128 ± 8 º. Upon the incorporation of SS protein, the PCL/SS scaffolds became more hydrophilic with contact angle of 106 ± 12 º (9:1), 75 ± 9 º (8:2), 42 ± 4 º (7:3), 0 º (6:4), and 0 º (5:5), respectively. The wettability of the PCL/SS fibers indicates that the hydrophilic macromolecule SS additive transforms the PCL, rendering its surface hydrophilic. This phenomenon due to the SS consists of 18 amino acids, most of which have strong polar side chains such as hydroxyl groups and its high hydrophilicity arises from the high content of serine and aspartic acid.[32]

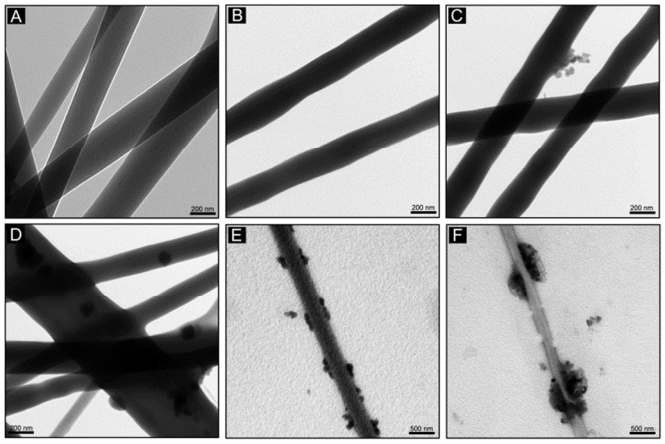

Figure 3. TEM images of the electrospun PCL/SS blend scaffolds with different weight ratios: (A) PCL; (B) PCL/SS 91; (C) PCL/SS 82; (D) PCL/SS 73; (E) PCL/SS 64; (F) PCL/SS 55.

We studied the morphology and structural properties of the scaffolds by FESEM and TEM (Fig. 2A–F and Fig. 3A–F). Fiber diameter was determined to be 648 ± 115 nm, 412 ± 88 nm, 402 ± 96 nm, 414 ± 112 nm, 502 ± 105 nm, and 586 ± 85 nm for pure PCL, PCL/SS 91, 82, 73, 64, and 55, respectively (Table 2). Partly, fiber diameter slightly decreased within the increase in the concentration of SS (10%, 20%, and 30%) in PCL/SS blends. This phenomenon could be due to the fact that the conductivity of blends solution with increase in the content of SS. SS is an amphiprotic macromolecule electrolyte.[32] More ions could be formed when we increase the SS content, leading to increased conductivity in blend solution. However, with increase SS wt% content (64 and 55 groups) produced non-uniform bead-fibers structures in the nanofibrous scaffolds. In our PCL/SS emulsion, the miscible polymers premixed prior to electrospinning produce a uniform phase distribution throughout the nanofibers, but this is not always case. When polymer content reaches a certain threshold (64 and 55 ratio), local domains of non-uniform mixed polymer can be formed.[42] To further verify this phenomenon of miscible SS and PCL components phases distribution, we used TEM to observe (Fig. 3E, F). In the TEM images, the higher SS content produced the bigger beads formation on the surface of the fibers. Therefore, controlling the concentration of SS content is very important for the formation of uniform PCL/SS nanofibers.

Table 2
Electrospinning conditions and results.

Component (w/w)	Solvent	Voltage (kV)	Fiber Diameter (nm)	Contact Angle (º)
PCL	HFIP	15	648 ± 115	128 ± 8
PCL/SS 91	HFIP/FA	16	412 ± 88	106 ± 12
PCL/SS 82	HFIP/FA	16	402 ± 96	75 ± 9
PCL/SS 73	HFIP/FA	18	414 ± 112	42 ± 4
PCL/SS 64	HFIP/FA	18	502 ± 105	0
PCL/SS 55	HFIP/FA	18	586 ± 85	0

3.2. Chemical and mechanical properties of PCL/SS nanofibrous scaffolds

To investigate chemical composition and conformational changes of SS in fibrous scaffolds after electrospinning, FTIR spectroscopy was performed (Fig. 4). The spectrum peaks of SS powder in the β-sheet include strong adsorption bands at 1626

cm^{-1} and 1518 cm^{-1}. Typical spectrum peaks for PCL and SS were observed in the spectroscopy of PCL/SS blend nanofibers. PCL include 1730 cm^{-1} (carbonyl stretching), 1294 cm^{-1} (C–O and C–C stretching) and 1239 cm^{-1} (asymmetric C–O–C stretching). However, after electrospinning, the spectrum peaks of SS in the β-sheet shifted from 1518 to 1527 cm^{-1}. Similarly, the amide I peak was shifted from 1626 to 1648 cm^{-1}, indicating that the content of β-sheet structure decreased. The specific mechanism of the transition is not clear, but our analysis of this phenomenon may be FA/HFIP solvent damaged the intermolecular hydrogen bond of SS in the process of dissolution.

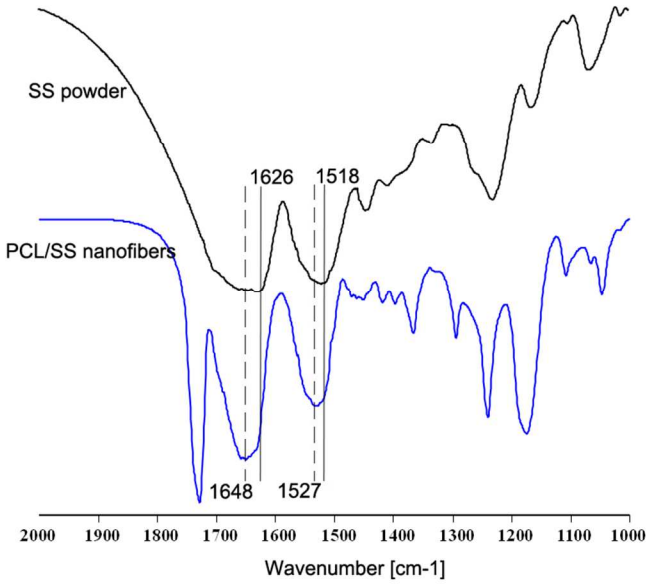

Figure 4. FTIR analysis of SS powder and electrospun PCL/SS nanofibrous scaffolds.

We further investigated the mechanical properties of PCL/SS nanofibrous scaffolds. From stress-strain curves, tensile strength and elongation at break were determined (Fig. 5). The PCL nanofibrous scaffold showed a very soft and flexible characteristic with low tensile strength at 5.6 ± 0.82 MPa and the high elongation at break of 182 ± 38%. For the PCL/SS blended fibrous scaffolds, as the SS content increased, the elongation at break decreased gradually (Fig. 5B). However, the tensile strength exhibited a noticeable behavior (Fig. 5A). PCL/SS 91 and 82 groups showed a significant enhanced tensile strength of 9.8 ± 1.54 MPa and 12.5 ± 2.1 MPa, respectively, which was increased about 2-3 times compared to that of PCL group. Furthermore, PCL/SS 91 and 82 groups still retained a relatively high elongation a break of 130 ± 15 % and 110 ± 16 %, respectively, thus having balanced strength and flexibility. However, there is a significantly decreased tensile strength and elongation at break in the PCL/SS 64 and 55 groups. In the SEM and TEM results (Fig. 2 and Fig. 3), we found that the higher SS content produced non-uniform structures, especially in PCL/SS 64 and 55 groups. The resulting PCL/SS phase inhomogeneites can lead to weak mechanical properties, particularly when the material size is reduced to the nano-scale.[43] Similar results were observed in electrospun PCL/collagen blends when the collagen component was raised to 70% (wt) and in a PLCL/collagen polyblend where the components were mixed in equal parts.[44, 45]

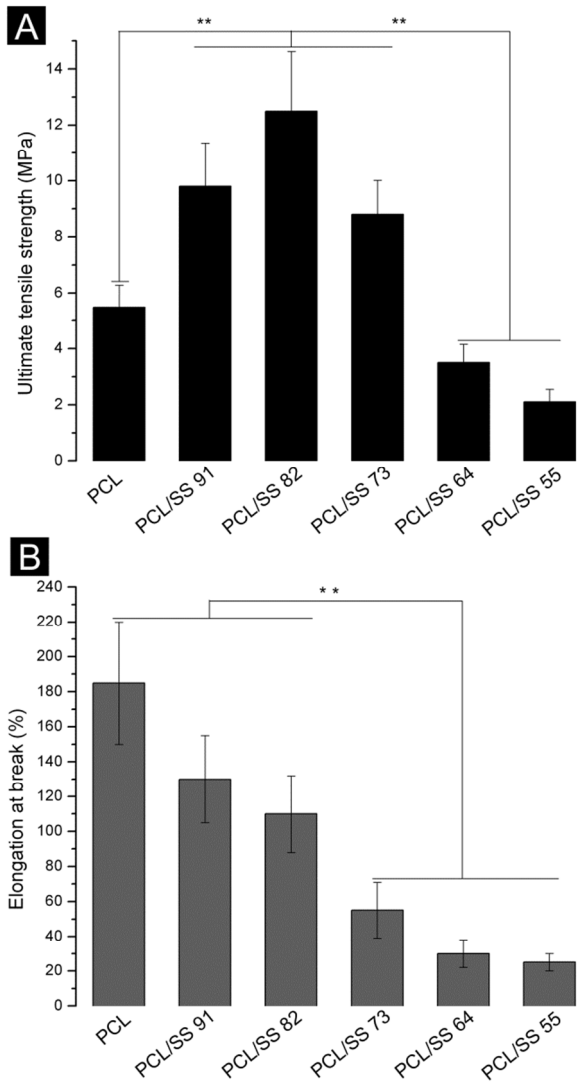

Figure 5. Mechanical properties of PCL, PCL/SS 91, 82, 73, 64, and 55 nanofibrous scaffolds. (A) ultimate tensile strength; (B) elongation at break. (** $p < 0.01$; Data presented are mean ± SD, n = 4).

3.3. *In vitro* FEK4 cells responses: cell morphology and proliferation

Electrospun nanofibrous scaffolds have been reported by several groups to mimic the natural ECM in the body and therefore to provide a preferable matrix for cell adhesion and proliferation.[46] Here, the effect of natural SS protein addition to PCL on cell adhesion and proliferation was investigated. According to structures of scaffolds by FESEM and TEM tests, we found a large number of non-uniform bead-fibers structures in PCL/SS 64 and 55 groups. This phenomenon will result in some uncertainty, e.g. with regards to changed surface topography and its influence on *in vitro* cell morphology and ECM expression. In this case, the structure-property-function relationships in PCL/SS nanofibers would become too complicated and difficult to interpret. Therefore, in the biological responses part (cell morphology and TGF-β1, collagen I, III expression), PCL/SS 64 and 55 groups were excluded.

FESEM images of human skin primary fibroblast cells (FEK4) cultured *in vitro* on the PCL, PCL/SS 91, 82, and 73 nanofibrous scaffolds for 1, 3 days are shown in Fig. 6. The FEK4 cells on

PCL/SS 91 scaffolds exhibited a more spreading morphology when compared to those on pure PCL scaffolds. Importantly, it was apparent that cells cultured on the 82 and 73 groups more elongated cellular morphology as compared to PCL and PCL/SS 91 scaffolds. Meanwhile, more filopodia protrusions were observed in 3day, revealing SS promotes protrusions outgrowth. The elongated cell filopodia extensions can bridge neighboring cells thereby enhancing the cell-cell interactions. Such morphology changes are often reported when cells such as fibroblasts were cultured on 3D ECM matrices reflecting a more physiological cellular microenviroment.[47] This observation indicates a better integration of fibroblasts with PCL/SS scaffolds, especially in the case of PCL/SS 82 and 73 groups.

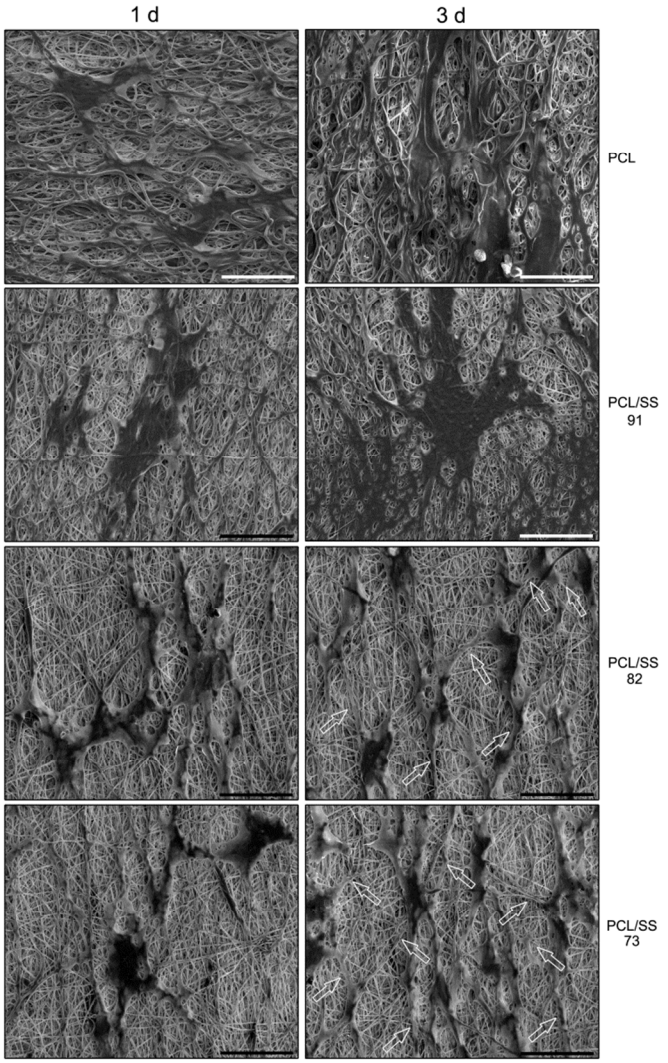

Figure 6. FESEM images of human primary skin fibroblasts (FEK4 cells) morphology on PCL, PCL/SS 91, 82, and 73 nanofibrous scaffolds for 1, 3 days. White arrows indicate the formation of filopodia protrusions in PCL/SS 82 and 73 scaffolds. Scale bar = 20 μm.

In addition to cell morphology, cell proliferation has been tested by MTS assay at 1, 3, 5 days. As shown in Fig. 7, there was a significant difference in the number of cells at the 1 and 3 days in the PCL, PCL/SS 91, and 82 groups between 64, and 55 groups. More hydrophobic groups might provide better cell adhesion and proliferation at the initial stage. After 5 days in culture, the cell numbers significantly increased in PCL/SS 91, 82, and 73 groups than those on PCL, PCL/SS 64, and 55 groups. These results indicate that the incorporation of SS into PCL at the appropriate ratio (PCL/SS 91, 82, and 73 groups) was beneficial for cell adhesion and proliferation. SS has been used to supplement serum-free media for the proliferation of various mammalian cells and in the protection of cells from acute serum deprivation.[25] Tsubouchi K. et al. also reported that SS enhanced human skin fibroblasts attachment and proliferation after 72 h culture.[23] On the other hand, the effect of surface wettability is largely to alter the type of the protein adsorption, which in turn affects cell adhesion and growth.[48, 49] Contact angles excessively high or low are not conductive to cell adhesion and growth. Therefore, our results suggest that PCL/SS in the appropriate ratio blends can enhance cell adhesion and proliferation, may depending on the inherent biochemical properties and surface wettability of PCL/SS nanofibrous scaffolds.

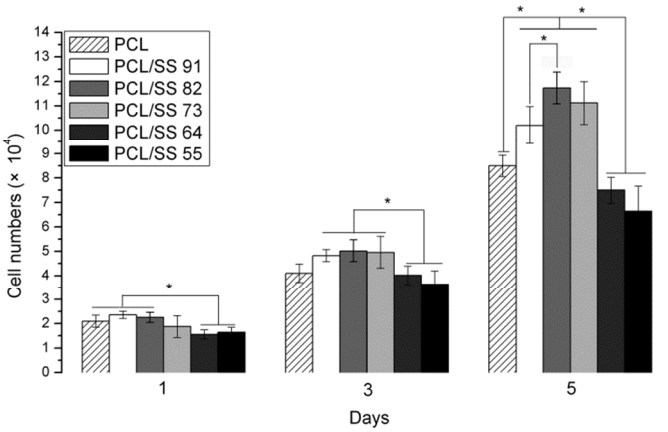

Figure 7. MTS assay for FEK4 cells proliferation on different scaffolds for 1, 3, 5 days (*p < 0.05; Data presented are mean ± SD, n = 5).

3.4. *In vitro* FEK4 cells responses: TGF-β1, collagen I, and collagen III expression

The goal of many tissue engineering approaches is to provide a framework for the assembly of natural ECM and growth factors secreted by resident cells *in vitro* and *in vivo*. For example, biodegradable tissue engineering scaffolds are designed to provide initial structural support that is intended to be replaced by naturally ECM as the original scaffolds degrade. Therefore, it is important that a good tissue engineering scaffold promotes ECM and growth factors production from resident cells. The results of the relative gene expression levels of TGF-β1, collagen type I and III for PCL, PCL/SS 91, 82, and 73 groups for 3 days are presented in Fig. 8. Real time RT-PCR confirmed that PCL/SS 82 and 73 groups significantly up-regulated the expression of TGF-β1 and collagen I as compared to PCL fibers. No significant difference was observed the expression of collagen III.

During the process of wound healing, TGF-β1 plays an important role. It is well established that TGF-β1 could induce fibroblast-to-myofibroblast differentiation independent of TGF-β1 signaling.[50] Meanwhile, TGF-β1 is a member of the transforming growth factor family and is known to play an important role in the regulation of ECM protein production.[51] Recent studies have illustrated that exogenous and endogenous TGF-β1 had the strong effect on the ECM proteins production of fibroblasts.[52, 53] In this study, we found that the gene expression of TGF-β1 and collagen I increased and cell morphology changes in SS-based nanofibrous scaffolds. These

results indicate SS component induced a higher level of TGF-β1 and collagen I gene expression may be contributed to cell shape changes. Previous study also showed that controlling cell shape through biomaterials can modulate the expression of TGF-β1 and ECM proteins.[52] Moreover, SS has been reported to promote collagen I production in a concentration-dependent manner.[54] Therefore, our results are consistent with the notion that cell shape and SS protein can mediate for TGF-β1 and collagen I production in connective tissue cells.

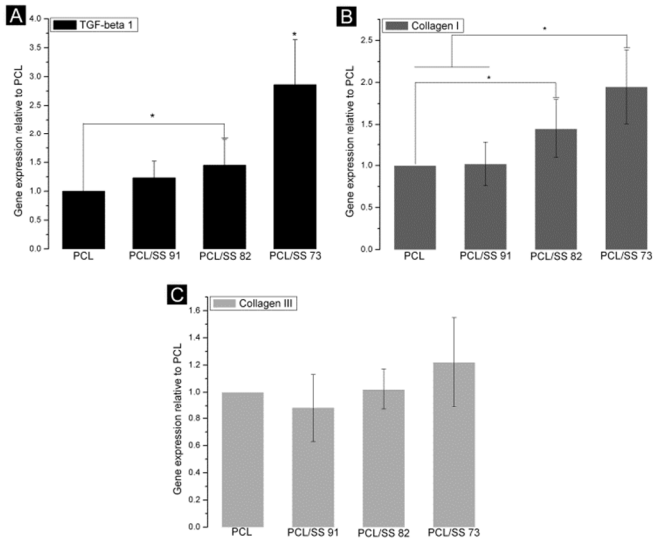

Figure 8. Real time RT-PCR analysis for gene expression levels of TGF-β1, collagen I, and collagen III on PCL, PCL/SS 91, 82, and 73 nanofibrous scaffolds for 3 days. Results were normalized to an endogenous control gene (GAPDH) and expression relative to PCL (*p < 0.05; Data presented are mean ± SD, n = 4).

3.5. *In vivo* host responses

To assess the host responses *in vivo*, each type of scaffolds was implanted subcutaneously in SD rats. After four weeks, we observed all nanofibrous scaffolds largely held their structural integrity *in vivo* (Fig. 9). We observed that most cells located on the surface of the PCL, PCL/SS 91, 82 groups. Interestingly, we found that increased penetration of cells into the PCL/SS 73 and 64 groups, this phenomenon may be contribute by SS degradation inducing increased the pore size of nanofibrous scaffolds. Importantly, the host responses consist of a series of complex reactions, recruitment of macrophages to the implanted scaffolds and fibrosis is characteristic of the early responses. The formation of fibrosis surrounding scaffolds can lead to loss of graft functions and medical complications.[55] In this study, we observed that there was no obvious difference of fibrosis thickness and the number of host cells response to tissue-scaffolds interface in the all groups.

Inflammation was assessed semi-quantitatively by the thickness of fibrous capsule and the presence of macrophages, and giant cells. We observed that SS-based scaffolds (especially in PCL/SS 82, 73) induced less recruited endogenous CD 68^{+} cell adhesion to the tissue-scaffolds interface compared to the PCL group (Fig. 10). This result suggested that the *in vivo* inflammatory response elicited by SS component was equivalent to or less than that observed on pure PCL nanofibrous scaffold. SS associated with the native silk fibers has been earlier implicated in immune response against the fiber.[56] However, Panilaitis et al. reported that there is a lack of inflammatory cells response to soluble SS protein, but SS coated fibroin fibers induced a stronger immune response than SS coated tissue culture plate.[57] The authors concluded that SS-mediated activation of the macrophages is dependent on its physical association with the fibroin resulting in a conformational change or better adhesion by the macrophages. *In vivo* experiments have also shown that SS does not have significant immunogenicity.[58, 59] Therefore, our results suggested that PCL/SS nanofibrous scaffolds should not cause seriously host responses.

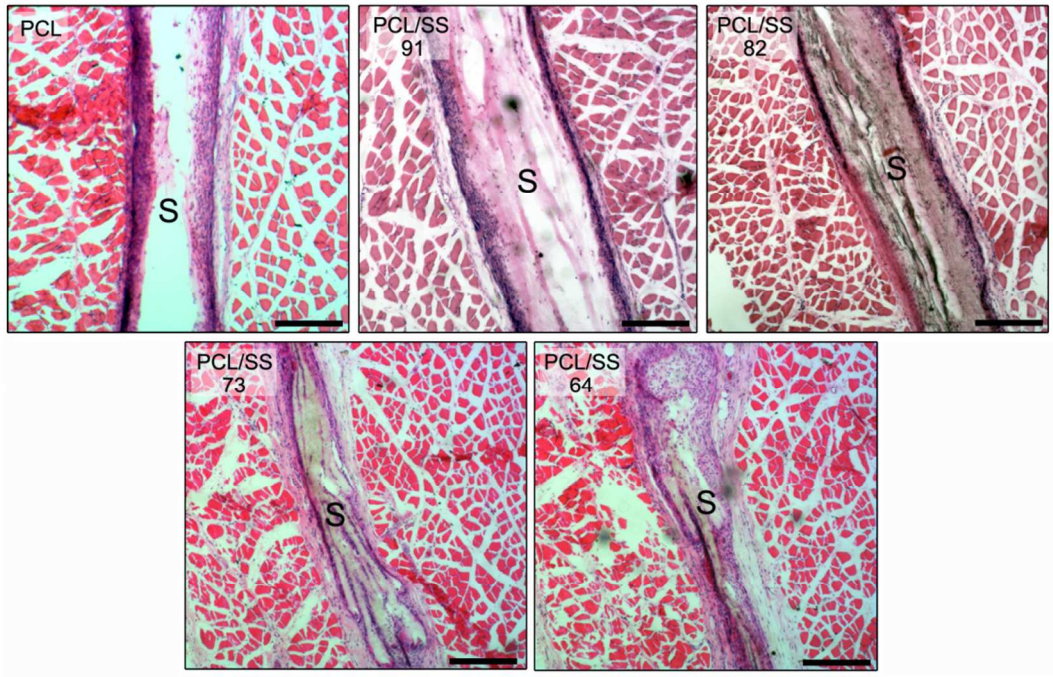

Figure 9. Representative images of hematoxylin/eosin staining of PCL, PCL/SS 91, 82, 73, and 64 nanofibrous scaffolds after 4 weeks subcutaneous transplanted. The scaffolds are labeled with "S". Scale bar = 500 μm.

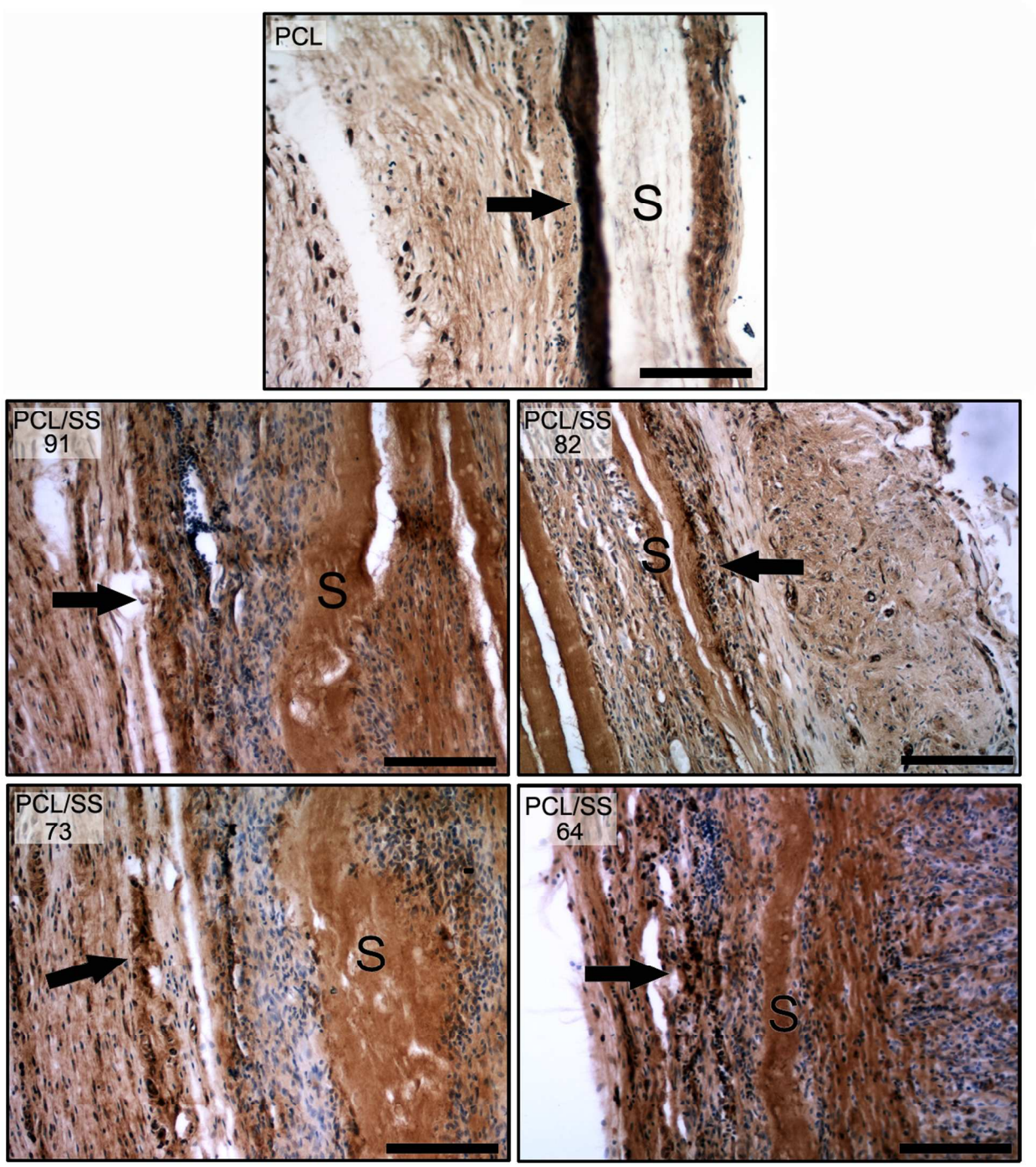

Figure 10. Representative images of immunohistochemistry CD68 staining of PCL, PCL/SS 91, 82, 73, and 64 nanofibrous scaffolds after 4 weeks subcutaneous transplanted. Black arrows (deep brown staining) indicate $CD68^{+}$ macrophages. The scaffolds are labeled with "S". Scale bar = 100 μm.

4. Conclusions

This study reports the successful fabrication of novel silk gland sericin protein /PCL nanofibrous scaffolds by emulsion electrospinning. The fiber morphology, mechanical properties, and wettability of PCL were modulated by incorporation of SS with various ratios of SS. In the appropriate ratio (especially in PCL/SS 91, 82, and 73 groups), the fabricated PCL/SS scaffolds greatly enhanced cell adhesion and proliferation. Meanwhile, SS component can up-regulate the gene expression of TGF-β1 and collagen I of human skin fibroblasts on the nanofibrous scaffolds. Furthermore, we confirmed by histology and immunohistochemistry that the *in vivo* host responses to PCL/SS blended scaffolds are similar to or less than pure PCL scaffold. These results demonstrate such a positive effect of SS, especially at the appropriate ratio, all on mechanical strength, bioactivity, and biocompatibility, would be potential application for tissue engineering scaffolds.

Acknowledgements

This work was supported by National Natural Science Foundation of China (11032012, 30870608), Key Science and Technology Program of CQ CSTC (CSTC, 2009AA5045), and Program for New Century Excellent Talents in University (NCET-10-0879). L. Li was supported by "China scholarship council 201206050045" and "Academic award for excellent Ph.D. candidates funded by ministry of education of China".

Notes and references

[a] Key Laboratory of Biorheological Science and Technology, Ministry of Education, Bioengineering College, Chongqing University, Chongqing 400030, China.

[b] Institute for Pharmacy and Food Chemistry, University of Wuerzburg, Am Hubland, DE-97074 Wuerzburg, Germany.

E-mail address: Yangli_cqu@163.com; Tel.: +86-023-65111802

1. R. Langer and J. P. Vacanti, *Science*, 1993, 260, 920-926.
2. F. Berthiaume, T. J. Maguire and M. L. Yarmush, *Annual review of chemical and biomolecular engineering*, 2011, 2, 403-430.
3. M. P. Lutolf and J. A. Hubbell, *Nat. biotechnol.*, 2005, 23, 47-55.
4. R. Langer and D. A. Tirrell, *Nature*, 2004, 428, 487-492.
5. Y. Gao, Z. Yang, Y. Kuang, M. L. Ma, J. Li, F. Zhao and B. Xu, *Biopolymers*, 2010, 94, 19-31.
6. T. D. Sargeant, M. O. Guler, S. M. Oppenheimer, A. Mata, R. L. Satcher, D. C. Dunand and S. I. Stupp, *Biomaterials*, 2008, 29, 161-171.
7. X. Liu and P. X. Ma, *Biomaterials*, 2009, 30, 4094-4103.
8. R. R. Duling, R. B. Dupaix, N. Katsube and J. Lannutti, *Journal of biomechanical engineering*, 2008, 130, 011006.
9. A. Greiner and J. H. Wendorff, *Angew. Chem.-Int. Edit.*, 2007, 46, 5670-5703.
10. D. Li and Y. N. Xia, *Adv Mater*, 2004, 16, 1151-1170.
11. N. Bhattarai, Z. Li, J. Gunn, M. Leung, A. Cooper, D. Edmondson, O. Veiseh, M. H. Chen, Y. Zhang and R. G. Ellenbogen, *Adv Mater*, 2009, 21, 2792-2797.
12. L. Ghasemi-Mobarakeh, M. P. Prabhakaran, M. Morshed, M. H. Nasr-Esfahani and S. Ramakrishna, *Biomaterials*, 2008, 29, 4532-4539.
13. A. J. Meinel, K. E. Kubow, E. Klotzsch, M. Garcia-Fuentes, M. L. Smith, V. Vogel, H. P. Merkle and L. Meinel, *Biomaterials*, 2009, 30, 3058-3067.
14. Y. Z. Zhang, J. Venugopal, Z. M. Huang, C. T. Lim and S. Ramakrishna, *Biomacromolecules*, 2005, 6, 2583-2589.
15. J. Gunn and M. Zhang, *Trends in biotechnology*, 2010, 28, 189-197.
16. C. Vepari and D. L. Kaplan, *Prog Polym Sci*, 2007, 32, 991-1007.
17. G. H. Altman, F. Diaz, C. Jakuba, T. Calabro, R. L. Horan, J. S. Chen, H. Lu, J. Richmond and D. L. Kaplan, *Biomaterials*, 2003, 24, 401-416.
18. L. Meinel, S. Hofmann, V. Karageorgiou, C. Kirker-Head, J. McCool, G. Gronowicz, L. Zichner, R. Langer, G. Vunjak-Novakovic and D. L. Kaplan, *Biomaterials*, 2005, 26, 147-155.
19. L. Meinel, V. Karageorgiou, S. Hofmann, R. Fajardo, B. Snyder, C. M. Li, L. Zichner, R. Langer, G. Vunjak-Novakovic and D. L. Kaplan, *J. Biomed. Mater. Res. Part A*, 2004, 71A, 25-34.
20. E. Wenk, H. P. Merkle and L. Meinel, *J Control Release*, 2011, 150, 128-141.
21. Y. Okazaki, S. Kakehi, Y. Xu, K. Tsujimoto, M. Sasaki, H. Ogawa and N. Kato, *Biosci Biotech Bioch*, 2010, 74, 1534-1538.
22. R. Dash, M. Mandal, S. K. Ghosh and S. C. Kundu, *Molecular and cellular biochemistry*, 2008, 311, 111-119.
23. K. Tsubouchi, Y. Igarashi, Y. Takasu and H. Yamada, *Biosci Biotech Bioch*, 2005, 69, 403-405.
24. S. Terada, T. Nishimura, M. Sasaki, H. Yamada and M. Miki, *Cytotechnology*, 2002, 40, 3-12.
25. M. Takahashi, K. Tsujimoto, H. Yamada, H. Takagi and S. Nakamori, *Biotechnol Lett*, 2003, 25, 1805-1809.
26. F. Zhang, Z. B. Zhang, X. L. Zhu, E. T. Kang and K. G. Neoh, *Biomaterials*, 2008, 29, 4751-4759.
27. S. Nayak and S. C. Kundu, *J. Biomed. Mater. Res. Part A*, 2013, 102, 1928-1940.
28. S. Nayak, T. Dey, D. Naskar and S. C. Kundu, *Biomaterials*, 2013, 34, 2855-2864.
29. K. S. Lim, J. Kundu, A. Reeves, L. A. Poole-Warren, S. C. Kundu and P. J. Martens, *Macromol. biosci.*, 2012, 12, 322-332.
30. B. B. Mandal, A. S. Priya and S. C. Kundu, *Acta biomater.*, 2009, 5, 3007-3020.
31. R. Dash, S. Mukherjee and S. C. Kundu, *Int J Biol Macromol*, 2006, 38, 255-258.
32. P. Aramwit, T. Siritientong and T. Srichana, *Waste management & research : the journal of the International Solid Wastes and Public Cleansing Association, ISWA*, 2012, 30, 217-224.
33. A. Cipitria, A. Skelton, T. R. Dargaville, P. D. Dalton and D. W. Hutmacher, *J Mater Chem*, 2011, 21, 9419-9453.
34. H. Teramoto, K. Nakajima and C. Takabayashi, *Biosci Biotech Bioch*, 2005, 69, 845-847.
35. P. Aramwit, S. Kanokpanont, T. Nakpheng and T. Srichana, *Int J Biol Macromol*, 2010, 11, 2200-2211.
36. H. Li, L. Li, Y. Qian, K. Cai, Y. Lu, L. Zhong, W. Liu and L. Yang, *Sheng Wu Yi Xue Gong Cheng Xue Za Zhi*, 2011, 28, 305-309.
37. L. Li, H. Li, Y. Qian, X. Li, G. K. Singh, L. Zhong, W. Liu, Y. Lv, K. Cai and L. Yang, *Int J Biol Macromol*, 2011, 49, 223-232.
38. S. U. Pham QP, Mikos AG., *Tissue Eng*, 2006 May, 12, 1197-1211.
39. S. Park, K. Park, H. Yoon, J. Son, T. Min and G. Kim, *Polym Int*, 2007, 56, 1361-1366.
40. S. Wongsasulak, K. M. Kit, D. J. McClements, T. Yoovidhya and J. Weiss, *Polymer*, 2007, 48, 448-457.
41. S. Chuangchote, T. Sagawa and S. Yoshikawa, *Jpn J Appl Phys*, 2008, 47, 787-793.
42. N. Bhattarai, Z. S. Li, J. Gunn, M. Leung, A. Cooper, D. Edmondson, O. Veiseh, M. H. Chen, Y. Zhang, R. G. Ellenbogen and M. Q. Zhang, *Adv Mater*, 2009, 21, 2792-2797.
43. J. Gunn and M. Q. Zhang, *Trends Biotechnol*, 2010, 28, 189-197.
44. H. M. Powell and S. T. Boyce, *Tissue Eng Pt A*, 2009, 15, 2177-2187.
45. I. K. Kwon and T. Matsuda, *Biomacromolecules*, 2005, 6, 2096-2105.
46. T. J. Sill and H. A. von Recum, *Biomaterials*, 2008, 29, 1989-2006.
47. E. Cukierman, R. Pankov and K. M. Yamada, *Curr Opin Cell Biol*, 2002, 14, 633-639.
48. D. Grafahrend, K. H. Heffels, M. V. Beer, P. Gasteier, M. Moller, G. Boehm, P. D. Dalton and J. Groll, *Nat Mater*, 2011, 10, 67-73.
49. J. D. Andrade and V. Hlady, *Adv Polym Sci*, 1986, 79, 1-63.
50. L. Vi, C. de Lasa, G. M. DiGuglielmo and L. Dagnino, *J Invest Dermatol*, 2011, 131, 586-593.

51. J. Massague, *Annu Rev Biochem*, 1998, 67, 753-791.
52. H. J. Shao, Y. T. Lee, C. S. Chen, J. H. Wang and T. H. Young, *Biomaterials*, 2010, 31, 4695-4705.
53. E. A. DesRosiers, L. Yahia and C. H. Rivard, *J Orthopaed Res*, 1996, 14, 200-208.
54. P. Aramwit, S. Kanokpanont, W. De-Eknamkul, K. Kamei and T. Srichana, *J Biomat Sci-Polym E*, 2009, 20, 1295-1306.
55. D. F. Williams, *Biomaterials*, 2008, 29, 2941-2953.
56. Y. Q. Zhang, *Biotechnol Adv*, 2002, 20, 91-100.
57. B. Panilaitis, G. H. Altman, J. S. Chen, H. J. Jin, V. Karageorgiou and D. L. Kaplan, *Biomaterials.*, 2003, 24, 3079-3085.
58. Y. Q. Zhang, Y. Ma, Y. Y. Xia, W. D. Shen, J. P. Mao and R. Y. Xue, *J Control Release*, 2006, 115, 307-315.
59. Y. Q. Zhang, M. L. Tao, W. D. Shen, J. P. Mao and Y. H. Chen, *J Chem Technol Biot*, 2006, 81, 136-145.

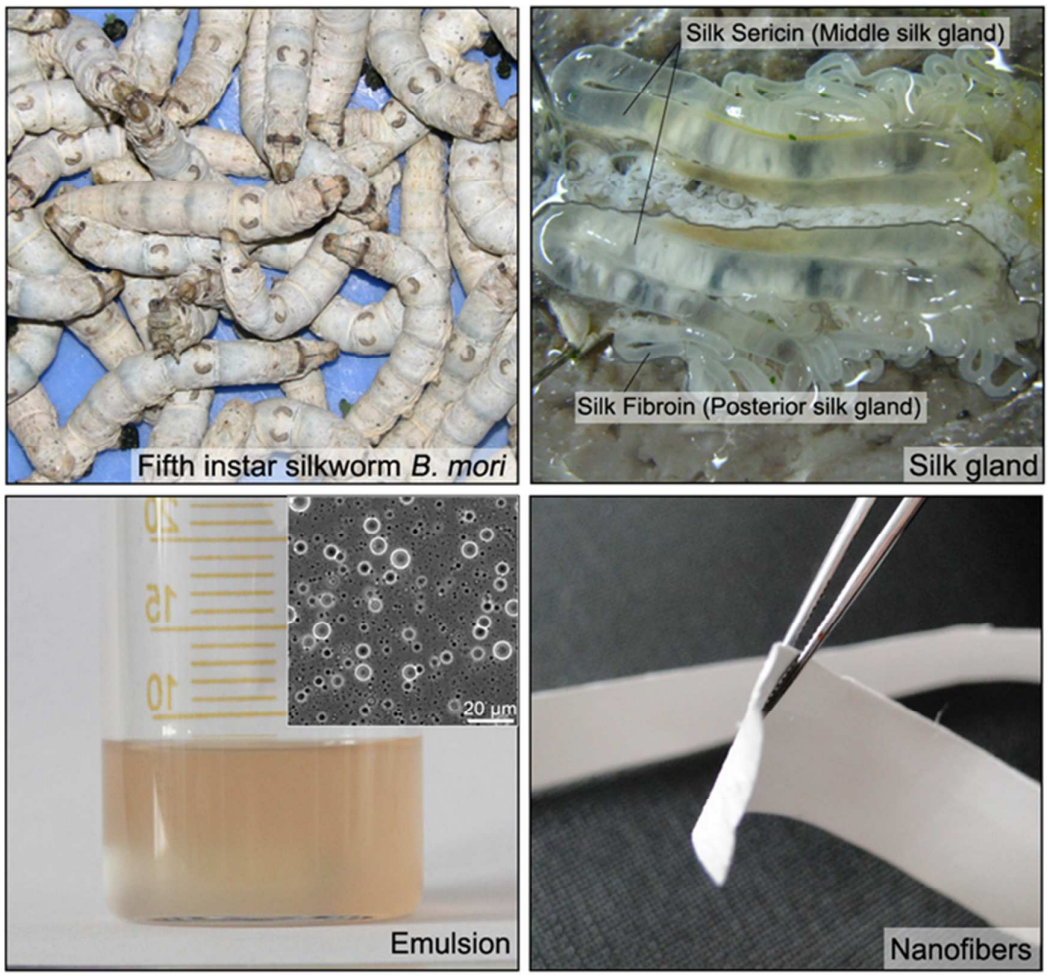

Silk middle gland extracted sericin protein based electrospun nanofibrous scaffolds with excellent biocompatibility have been developed for tissue engineering applications.